

This article was downloaded by:

On: 25 January 2011

Access details: *Access Details: Free Access*

Publisher *Taylor & Francis*

Informa Ltd Registered in England and Wales Registered Number: 1072954 Registered office: Mortimer House, 37-41 Mortimer Street, London W1T 3JH, UK



## Liquid Crystals

Publication details, including instructions for authors and subscription information:

<http://www.informaworld.com/smpp/title~content=t713926090>

### Frustrated smectic phases in swallow-tailed compounds with perfluorinated chains

D. Lose; S. Diele; G. Pelzl; E. Dietzmann; W. Weissflog

Online publication date: 06 August 2010

**To cite this Article** Lose, D. , Diele, S. , Pelzl, G. , Dietzmann, E. and Weissflog, W.(1998) 'Frustrated smectic phases in swallow-tailed compounds with perfluorinated chains', *Liquid Crystals*, 24: 5, 707 – 717

**To link to this Article:** DOI: 10.1080/026782998206821

**URL:** <http://dx.doi.org/10.1080/026782998206821>

PLEASE SCROLL DOWN FOR ARTICLE

Full terms and conditions of use: <http://www.informaworld.com/terms-and-conditions-of-access.pdf>

This article may be used for research, teaching and private study purposes. Any substantial or systematic reproduction, re-distribution, re-selling, loan or sub-licensing, systematic supply or distribution in any form to anyone is expressly forbidden.

The publisher does not give any warranty express or implied or make any representation that the contents will be complete or accurate or up to date. The accuracy of any instructions, formulae and drug doses should be independently verified with primary sources. The publisher shall not be liable for any loss, actions, claims, proceedings, demand or costs or damages whatsoever or howsoever caused arising directly or indirectly in connection with or arising out of the use of this material.

# Frustrated smectic phases in swallow-tailed compounds with perfluorinated chains

by D. LOSE, S. DIELE\*, G. PELZL, E. DIETZMANN and W. WEISSFLOG  
 Institut für Physikalische Chemie, Martin-Luther-Universität, Halle-Wittenberg,  
 Mühlpforte 1, 06108 Halle/S., Germany

(Received 4 August 1997; in final form 6 November 1997; accepted 26 November 1997)

A group of 4-[4-(4-*n*-octyloxybenzoyloxy)benzoyloxy]benzylidenemalonic acid bis(perfluoralkyl) esters and 4-{4-[2,2-bis(*n*-octyloxycarbonyl)ethenyl]benzoyloxy}benzoic acid 4-perfluoroalkoxyphenyl esters with varied lengths of the perfluorinated chains were investigated by X-ray measurements. The liquid crystalline behaviour (SmA, SmC, Col) and the structures of the phases are described. The substances show the influence of the steric interaction caused by the wedge shape of the molecules and the repulsion caused by chemically incompatible segments (fluorophobic effect). In the first group of compounds investigated the steric interaction clearly dominates the structure, so that an antiparallel packing of the molecules in SmA and SmC phases results. In the second group, the influence of the incompatibility is more and more enhanced and a low temperature phase with a columnar structure arises in which the incompatible parts are separated on a microscopic scale.

## 1. Introduction

The covalent linking of chemically incompatible moieties (in this case the combination of perfluorinated moieties with aromatic and aliphatic moieties) is an actual way to vary or to create new liquid crystalline structures. The most simple chemical structure can be found in semifluorinated alkanes which exhibit liquid crystalline properties [1–6]. Even these simple compounds form smectic phases with structural peculiarities. The different parts of the molecules are assumed to be organized in different sub-layers. Today, a lot of partially fluorinated compounds are known, all of which show that minor changes of the chemical structure can lead to essential differences in the packing of the molecules [7–21]. One significant parameter is the ratio of the smectic layer thickness to the length of the molecules. Values of the ratio between 0.7 [22] and 1.7 [16] are known, proving the existence of SmA<sub>1</sub> and SmA<sub>d</sub> phases. In well oriented samples the existence of a periodicity perpendicular to the layer normal can also be detected (undulated structures) which leads to the two-dimensional SmA or SmC phases [7, 16].

These results are in strong analogy to the smectic phases of terminally polar substances, in which these structure types were discovered [23] and theoretically explained [24, 25]. Different types or sub-groups of smectic phases can be achieved, too, in the case of molecules with a strong asymmetric shape. The additional steric inter-

action leads to a frustration of the packing in the smectic layers. The influence of the molecular shape was extensively studied years ago by introducing so-called steric dipoles or steric quadruples [26, 27]. In lateral aryl-substituted mesogens, periodicities incommensurable to the layer period of the SmA phase have been found [28]. In tuning fork-like substances, transitions within the SmA and SmC phase could be proved [29]. Therefore it can be stated that an additional intermolecular interaction—such as terminal dipoles, steric asymmetry or chemical incompatibility—forces the appearance of new phases.

In the present paper we present wedge-shaped compounds with perfluorinated units in different positions. These molecules show a strong steric asymmetry, and on the other hand they contain incompatible molecular moieties. Both the steric asymmetry and the chemical incompatibility here play an important role in structure formation.

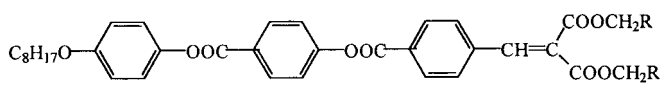
## 2. Experimental

The synthetic routes to the substances under discussion have been described earlier [30]. The phase behaviour of the substances studied is given in table 1.

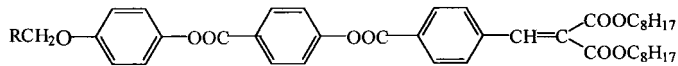
The phase transitions were studied using a differential scanning calorimeter (DSC Perkin Elmer) and a polarizing microscope (Leitz Orthoplan) equipped with a Linkam hot stage. The X-ray diffraction patterns of non-oriented samples were recorded using the Guinier method. Well developed monodomains could be achieved

\* Author for correspondence.

Table 1. Structural formulae, phase transition temperatures ( $^{\circ}\text{C}$ ), code names, molecular lengths and layer spacings.  $L$  = length of molecules measured by CPK-models (the most stretched conformation);  $d^A$ ,  $d^C$ ,  $d^{\text{Col}}$  = layer spacing;  $\alpha$  = maximal tilt angle of the molecules with respect to the layer normal.

			$L/\text{nm}$	$d^A/\text{nm}$	$d^C/\text{nm}$ ( $\alpha^{\circ}$ )	$d^{\text{Col}}/\text{nm}$ ( $\alpha^{\circ}$ )
A	R					
<b>A0</b>	$\text{C}_7\text{H}_{15}$	Cr 40 SmC 51 N 88 I	4.5	—	3.8 (~30)	—
<b>A1</b>	$\text{C}_3\text{F}_7$	Cr 127 (SmC 122) SmA 130 N 134 I	4.08	3.8	3.65 (16)	—
<b>A2</b>	$\text{CH}_2\text{C}_6\text{F}_{13}$	Cr 116 SmC 153 SmA 161 I	4.62	4.28	3.98 (22)	—
<b>A3</b>	$\text{C}_7\text{F}_{15}$	Cr 119 SmC 137 SmA 143 N 146 I	4.62	4.36	4.1 (20)	—

						
B						
<b>B1</b>	$\text{C}_3\text{F}_7$	Cr 43 SmC 63 SmA 99 I	4.08	3.53	3.4 (16)	—
<b>B2</b>	$\text{CH}_2\text{C}_6\text{F}_{13}$	Cr 67 Col 69 SmC 79 SmA 151 I	4.62	4	3.7 (22)	7(29)
<b>B3</b>	$\text{C}_7\text{F}_{15}$	Cr 60 (Col 54) SmC 66 SmA 150 I	4.62	4	3.7 (22)	7(29)
<b>B4</b>	$\text{CH}_2\text{C}_8\text{F}_{17}$	Cr 98 Col <sub>rec</sub> 99 SmA 175 is	4.88	4.3	—	7.5(0)
<b>B5</b>	$\text{C}_9\text{F}_{19}$	Cr 85 (Col <sub>rec</sub> 74) SmX 88 SmA 173 I	4.88	4.34	—	7.5(0)
<b>B6</b>	$\text{C}_{11}\text{F}_{23}$	Cr 109 Col <sub>rec</sub> 112 SmA 185 I	5.08	4.5	—	7.96(0)

by surface alignment on a glass plate; the incident beam was nearly parallel to the glass plate. The scattering from oriented samples was measured using a two-dimensional area detector (HI-STAR detector, Siemens). The sample-detector distance could be varied between 90 and 250 mm. Because of the scattering geometry used, only the upper half of the reciprocal space could be detected; the lower half was shadowed by the glass plate. To check the symmetry of the full pattern, oriented samples in glass capillaries were used, but the alignment was generally not of such high quality. The temperature stabilization during the measurements was better than 0.2 K.

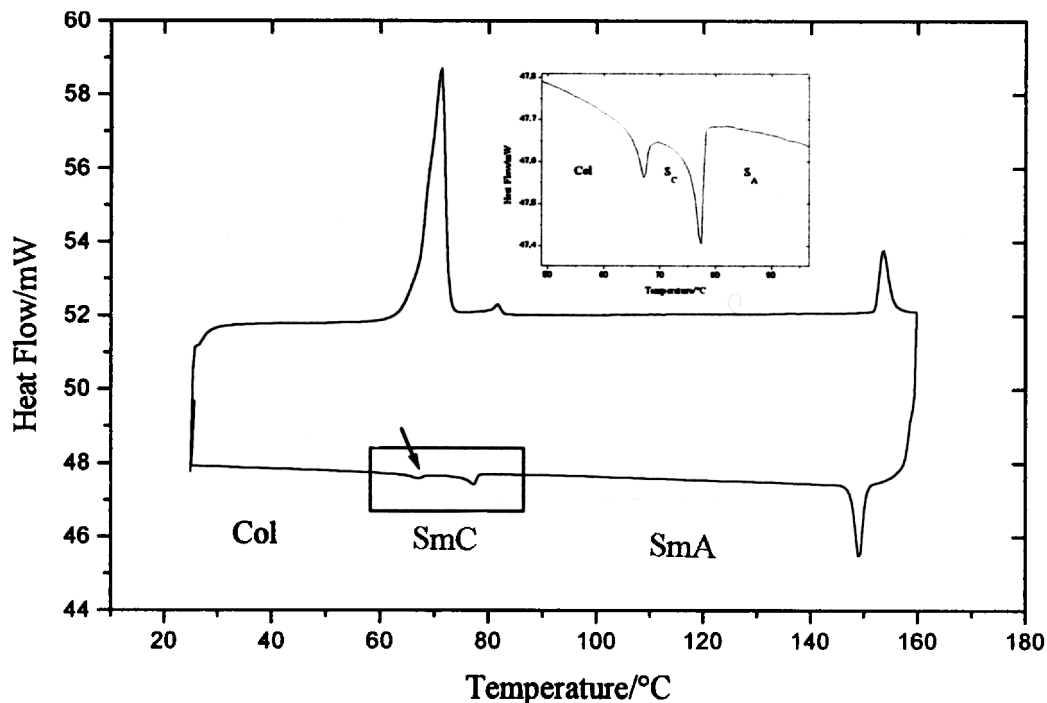
### 3. Results

The liquid crystalline phases were assigned from their textures. The SmA phases exhibit the typical fan-shaped texture or homeotropic texture, whereas the SmC phase mostly appears as a schlieren texture. The mesophases below the SmC phase (previously designated by SmX and in the following proved to be a columnar phase) could not be distinguished from the SmC phase by texture observations. But a clear peak in the DSC trace (figure 1) indicates the transition. In the case of compound **B6**, the transition between the SmA and Col<sub>rec</sub> phase is clearly connected with a texture change (figure 2). According to their polymorphism the substances can be divided into three groups. Compounds

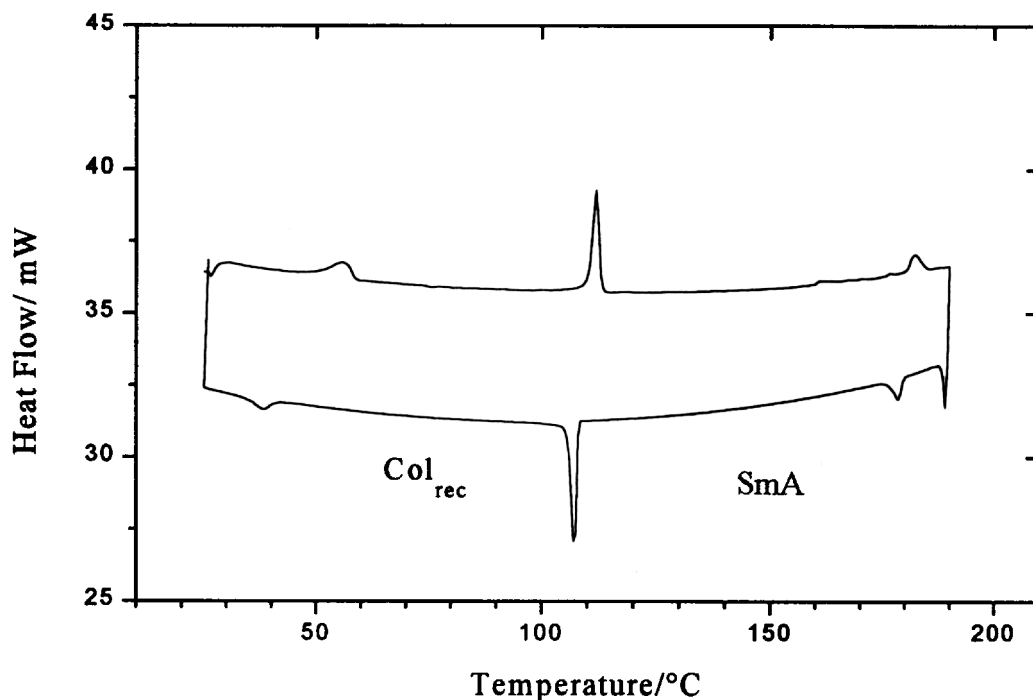
**A1–A3** and **B1** exhibit a smectic dimorphism SmC, SmA and an additional nematic phase (**A1**, **A3**). In the second group (**B2**, **B3**), the smectic dimorphism is observed and additionally a low temperature phase. In the third group (**B4**, **B5**, **B6**), only a smectic phase (SmA) besides the low temperature phase is found. The low temperature phase can be easily supercooled to room temperature. Each group contains its own structural peculiarities which are discussed below. The above phase behaviour of the compounds is supported by the X-ray studies.

#### 3.1. Compounds **A1**, **A2**, **A3** and **B1**

In the first group the known X-ray patterns of the SmA and SmC phase are observed, this meaning the first and second order of the layer reflection together with a diffuse scattering around a Bragg angle of  $9^{\circ}$  as shown for compound **B1** [figure 3(a)]. The  $d$ -values decrease continuously below the SmA  $\rightarrow$  SmC transition indicating an inclination of the molecules [figure 4(a)]. A maximal tilt angle calculated according to  $\alpha = \cos^{-1} d^C/d^A$  is about  $20^{\circ}$  (table 1). The layer thickness in the SmA phase corresponds to the length of the molecules. Obviously the fluorination of the terminal branched chains increases the steric asymmetry of the molecules and encourages the antiparallel packing of the molecules (**A1**, **A2**, **A3**) which has already been described for the non-fluorinated analogues [31, 32]. Also the fluorination of the short non-branched chain



(a)



(b)

Figure 1. DSC curves of compounds **B2** (a) and **B6** (b), heating and cooling rate  $10 \text{ K min}^{-1}$ . Arrowed area in (a) is expanded in the inset:  $\Delta H_{\text{SmC-Col}} = 0.25 \text{ J g}^{-1}$ . In (b)  $\Delta H_{\text{SmA-Col}} = 10 \text{ J g}^{-1}$ .

at the other end of the molecule (**B1**) is too weak to change the antiparallel packing. Therefore an antiparallel structure of the wedge-shaped molecules in a smectic  $A_1$  type can be derived in which the fluorinated

and non-fluorinated moieties are arranged together. This can be related to miscibility studies [33–35], in which short perfluorinated chains are found to be miscible with hydrogenous aliphatic chains.

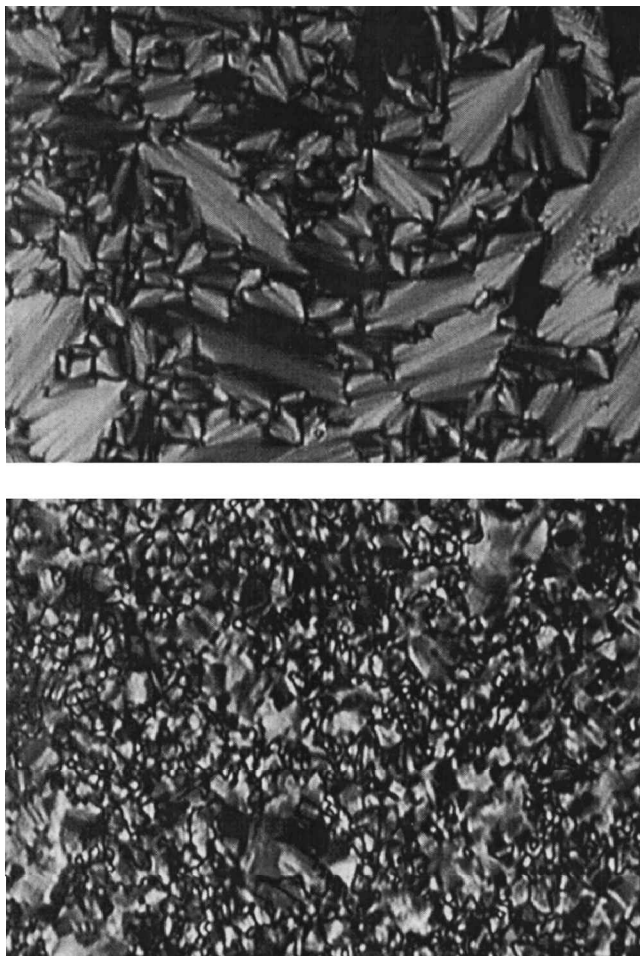


Figure 2. Textures of compound **B6**. Top: SmA phase (140°C). Lower: Col<sub>rec</sub> phase (100°C).

### 3.2. Compounds **B2** and **B3**

In the second group, the feature of the X-ray patterns is quite different. The pattern of non-oriented samples [**B2**, figure 3(b)] exhibits a layer reflection of extremely low intensity. Simultaneously a strong diffuse scattering in the small angle region appears which sometimes covers the layer reflection. The diffuse scattering condenses to Bragg reflections in the small angle region at the transition into the columnar phase (below the SmC phase).

The wide angle scattering remains unchanged (maximum around 9.5°) in the SmA and SmC phases. The temperature dependence of the *d*-values in the SmA and SmC phases exhibits the same behaviour as that found for the compounds of the first group, and a discontinuous change of the *d*-value at the transition into the low temperature phase could not be detected [figure 4(b)]. This implies that in this phase too the molecules must be tilted with respect to the layer normal. The *d*-value in the SmA phase corresponds to the length

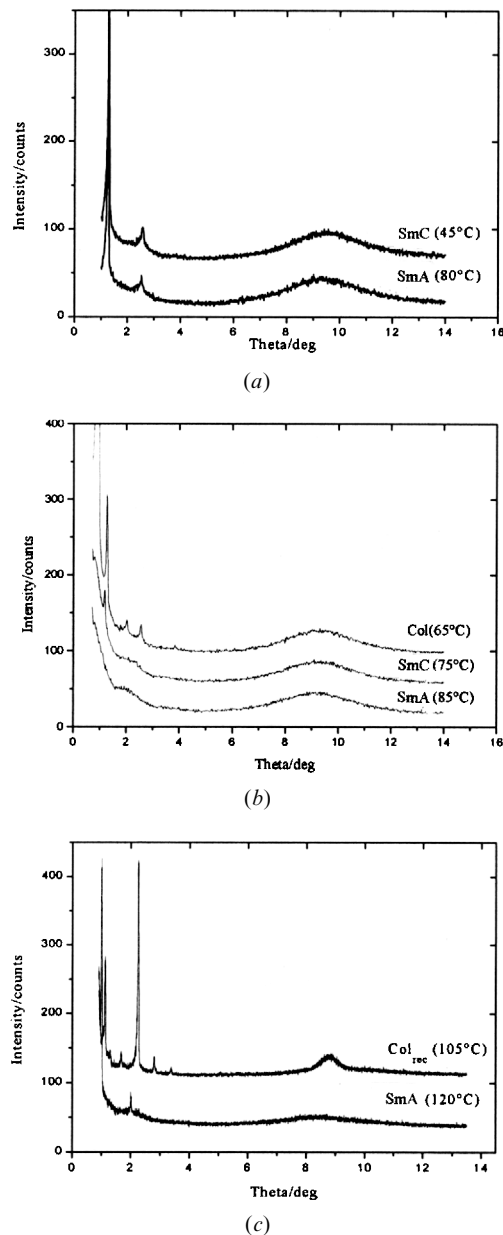
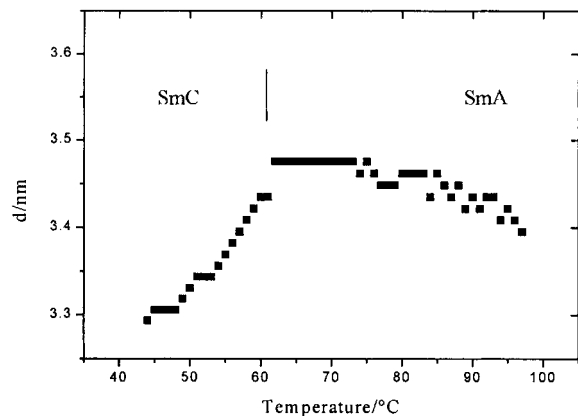


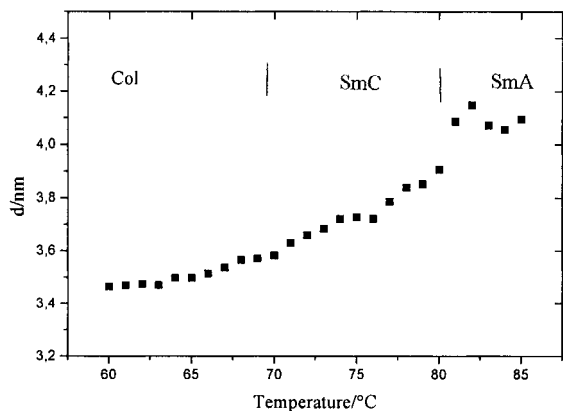
Figure 3. X-ray diffraction patterns of non-oriented samples of compounds **B1** (a), **B2** (b) and **B6** (c).

of the molecules which can be explained by a monolayer packing of antiparallel aligned molecules [figure 5(a)]. However the strong diffuse scattering in the small angle region indicates the existence of a molecular organization with a bimolecular length, as found in the low temperature phase, but without long range order.

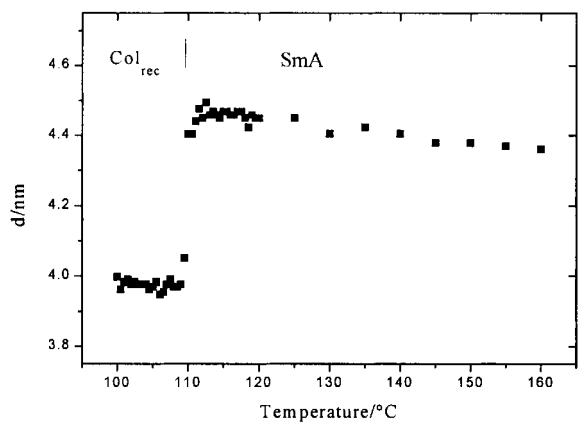
The outer diffuse scattering in the low temperature phase exhibits an asymmetric profile which has been analysed as consisting of two maxima at 8.9° and 10.3° [figure 6(a)]. The wide angle scattering of the equivalent non-fluorinated compound shows only one diffuse scattering with a maximum at 10.2° [figure 6(c)]. This



(a)



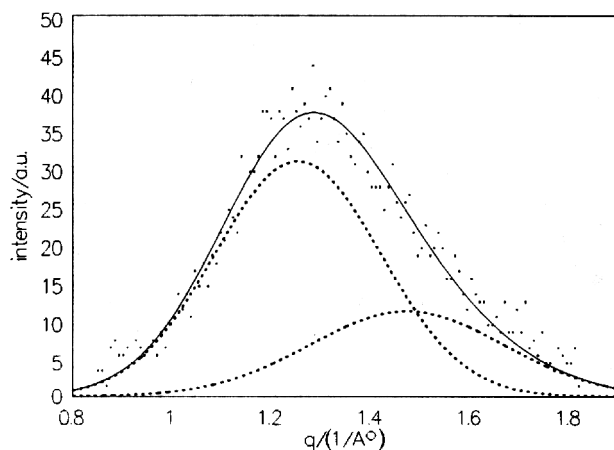
(b)



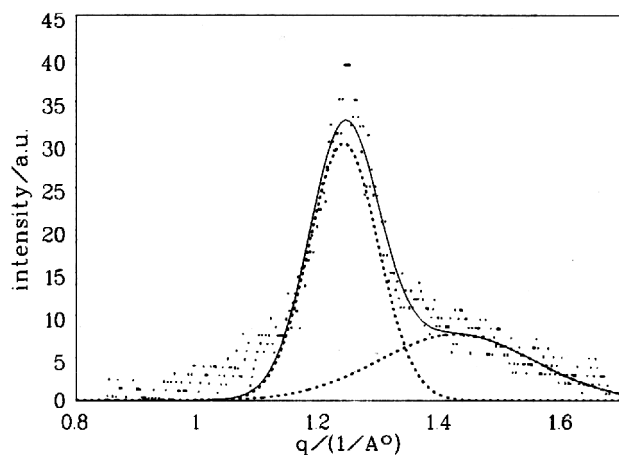
(c)

Figure 4. Layer-spacing  $d$  as a function of temperature of compounds **B1** (a), **B2** (b) and **B6** (c).

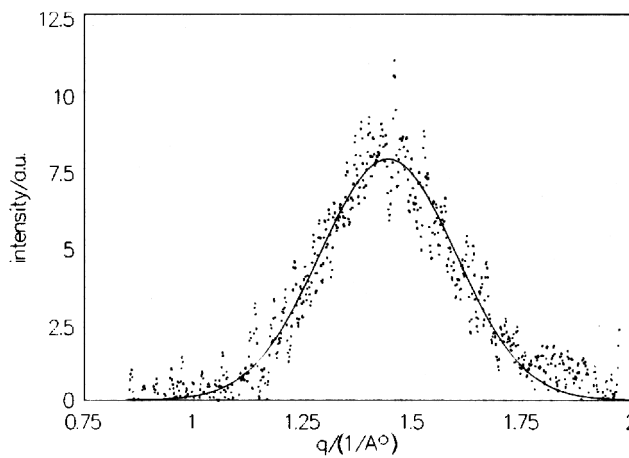
maximum is commonly observed for aliphatic or aromatic parts, whereas for perfluorinated chains the maximum is detected about  $8\text{--}9^\circ$  [36–38]. These values were attributed to the disordered state of the aliphatic and perfluorinated chains, respectively. Therefore the first observed wide angle scattering is caused by the perfluorinated moieties and the second by the aliphatic



(a)



(b)



(c)

Figure 6. Comparison of the profiles of the wide angle scattering in the low temperature phase of compounds **B2** (a) and **B6** (b) and for comparison in the SmC phase of compound **A0** (c) ( $q = 2\pi/d = 4\pi/\lambda \sin \theta$ ).

and aromatic regions. This result points to a layer structure in which the chemically incompatible parts are segregated in different sub-layers.

The patterns of the well oriented samples support these results (figure 7). In the small angle region of the pattern for the SmA and SmC phase, a weak layer reflection at the meridian of the pattern and two diffuse scattering maxima (1st and 2nd order) can be detected [figure 7(a) and 7(b)]. Figure 8 displays the development of the diffuse scattering as a function of the angle  $\chi$ , where  $\chi$  is the angle between the layer normal and the position of the maxima. Approaching the low temperature phase, the diffuse scattering becomes more and more concentrated out of the meridian, but the positions of the maxima remain constant. The maxima condense to Bragg-spots shown in figure 7(c). The arrangement of

the reflections on the pattern of the oriented sample suggests the assumption of a rectangular centred cell. The lattice parameter as well as the reflections calculated on the basis of this assumption are listed in table 2(a). The agreement between calculated and measured values is very good.

To explain the experimental results by a structural model, the different cross-sections  $\delta$  of different parts ( $\delta_{Ar}=0.22\text{ nm}^2$  aromatic,  $\delta_F=0.28\text{ nm}^2$  perfluorinated and  $\delta_{Alk}=0.18\text{ nm}^2$  aliphatic moieties) [39–43] of the molecule must be considered. To prevent ‘holes’ in the packing, the differences can be equalized by a tilt  $\psi$  of the different moieties [44, 45] with respect to each other [figure 9(a)]. According to  $\delta_F/2\delta_{Alk} = \cos \psi$  the perfluorinated moieties form an angle of  $33^\circ$  and the aromatic parts an angle of  $52^\circ$  ( $\delta_{Ar}/2\delta_{Alk} = \cos \psi$ ). With

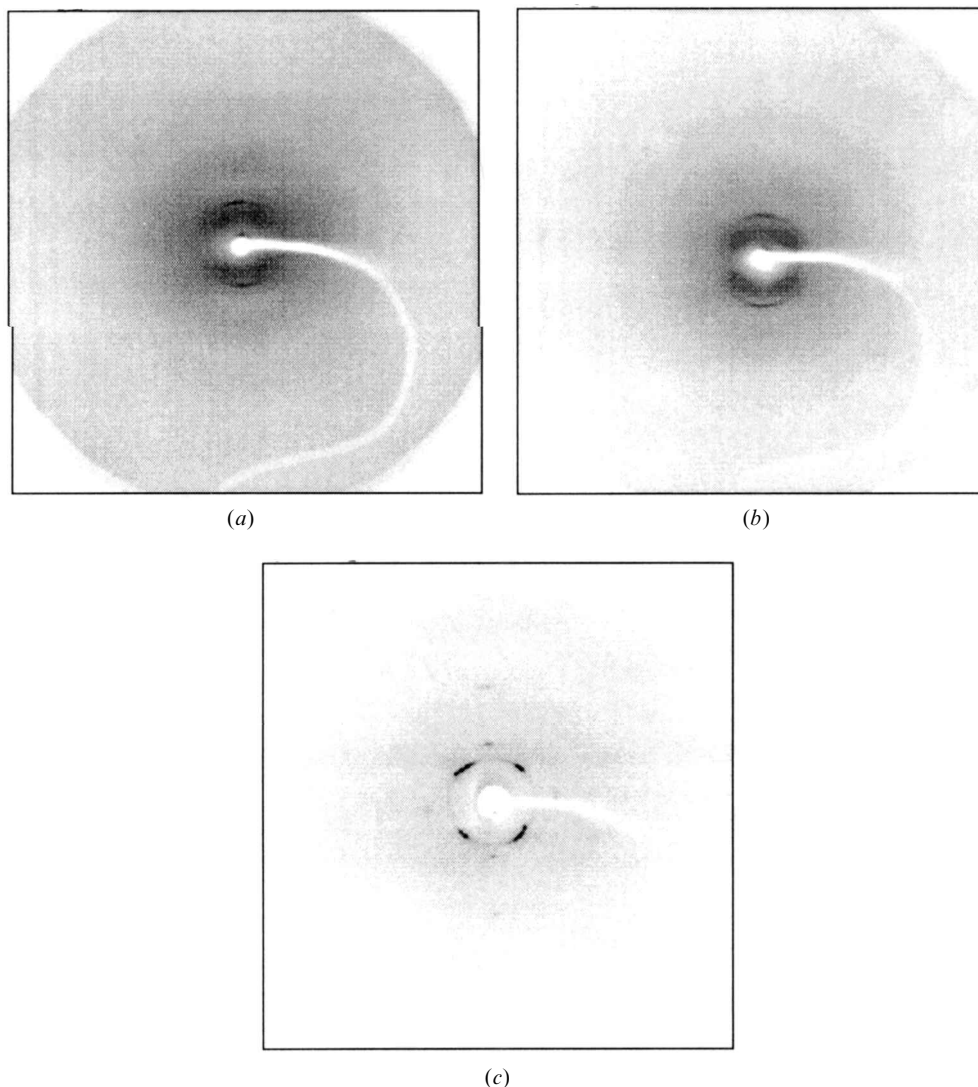


Figure 7. X-ray patterns of the small angle region of the oriented sample of compound **B2**. SmA phase at  $130^\circ\text{C}$  (a); SmC phase at  $75^\circ\text{C}$  (b); Col phase at  $65^\circ\text{C}$  (c).

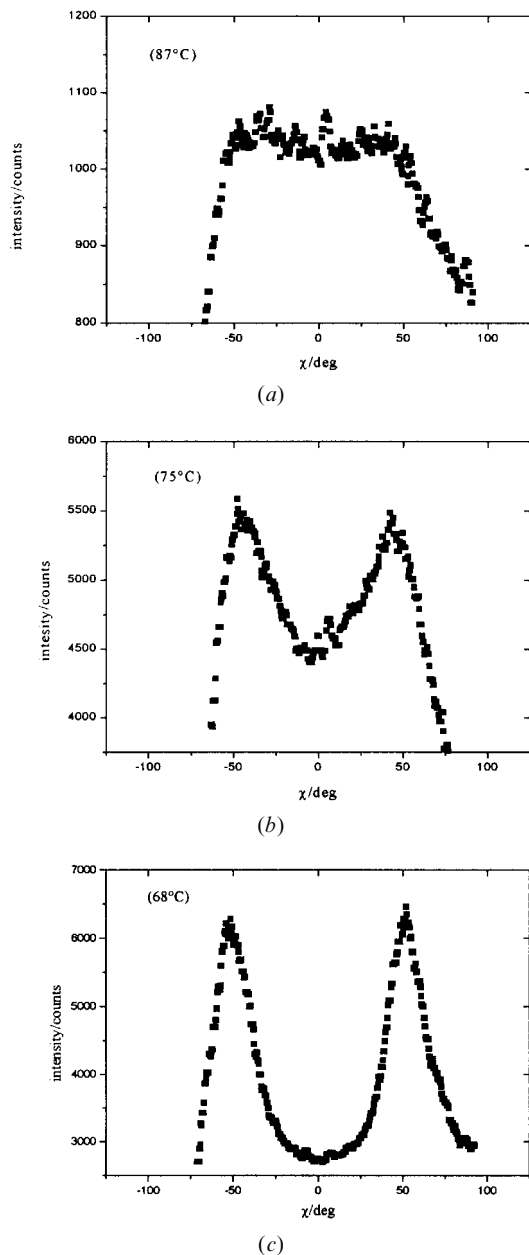


Figure 8. Development of the diffuse small angle scattering of compound **B2** as a function of  $\chi$  ( $\chi$  is the angle between the layer normal and the position of the maxima). SmA phase (a); SmC phase (b); Col phase (c).

respect to the molecular long axis, the aliphatic chains are tilted by about  $52^\circ$  and the fluorinated chain by about  $19^\circ$ . With these tilt angles and the length of the moieties (figure 9), the molecular length is calculated to be  $L = 4.1$  nm which is in a good agreement with the measured  $d$ -value in the SmA phase.

In the SmC phase a tilt angle of about  $22^\circ$  is measured on the basis of oriented samples. Cooling the sample into the low temperature phase, the tilt of the molecules with respect to the layer normal is increased ( $29^\circ$ ), but

the pattern is now explained by a two-dimensional centred rectangular lattice [table 2, figure 5(b)] built up of fragments of layers in which the molecules are tilted. The translation period  $b$  in the direction of the layer normal indicates that the molecules are organized in a double layer so that fluorinated and non-fluorinated parts are separated. To reconcile the structural model shown in figure 5(b) with the condition of a two-dimensional centred cell (which means the presence of a glide mirror plane) the building group in the centre must be rotated around the  $c$  axis by  $180^\circ$ . That would be compatible with the disordered structure. Since the experimental conditions do not allow us to distinguish between a rotational disorder of the whole sample (fibre symmetry) and the above mentioned alignment of the building groups, an alternative evaluation of the pattern is added based on the assumption of a two-dimensional oblique lattice. In this model [figure 5(c)] the rotation of the centred building group is not necessary. The re-indexing of the pattern, as in table 2(b), and the derived lattice do not alter the conclusions discussed with respect to the molecular packing.

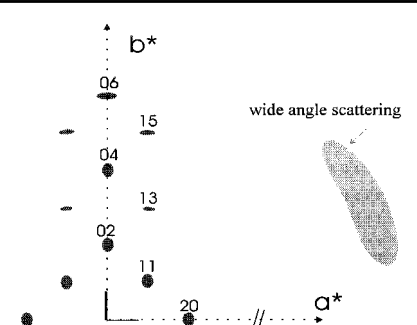
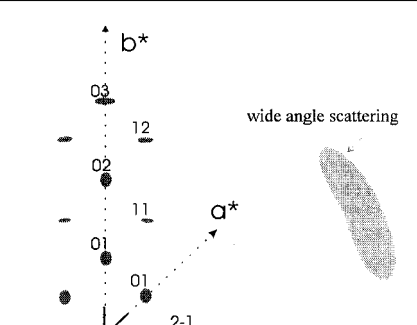
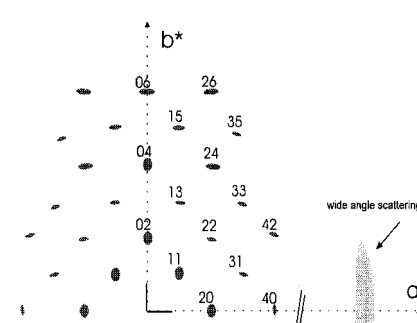
### 3.3. Compounds **B4**, **B5** and **B6**

In the third group, the perfluorinated part is increased in size and a different phase behaviour is found (table 1). The SmA phase directly passes over into the columnar phase [figures 3(c) and 4(c)]. The patterns of the oriented sample (figure 10) show the typical feature of the SmA phase and a layer spacing of the SmA, structure ( $d \approx L$ ) is observed. The tilt  $\psi$  of the molecular moieties with respect to each other is the same as described above (compounds **B2/B3**) and explains the  $d$ -value ( $d^A = 4.4$  nm).

Approaching the transition into the low temperature phase, a diffuse scattering besides the pronounced layer reflection in the small angle region [figure 10(b)] indicates again an undulation of the smectic layers on a short range scale. On cooling the sample numerous spot-like reflections are detected in the small angle range and these have been indexed on the basis of a two-dimensional rectangular centred cell [figure 10(c)]. The apparent splitting of the equatorial reflections can be explained—in our opinion—by the sample preparation on the glass plate and it is not generally observed at the pattern of this phase. An interpretation in terms of a twinning with an oblique cell with an angle between the axes of about  $85^\circ$  could be taken into consideration too, but it would demand that the numerous observed ( $hk$ ) reflections with  $k \neq 0$  should also be split, which can be excluded with certainty. It is remarkable that the ( $h0$ ) reflections on the equator of the pattern could be detected too, a feature which up to now has never been observed in other systems. This may be due to the higher



Table 2. Scheme of the X-ray patterns (columnar phases) of compounds **B2** (a) and (b) and **B6** (c); observed and calculated reflections, Miller indices of the two-dimensional lattice. (a) and (b) display two alternative indexings of the same pattern (rectangular and oblique, respectively).

(a) <b>B2</b> Col <sub>rec</sub>	$\theta_{\text{exp}}$	$hk$	$\theta_{\text{cal}}$
	0.97	11	—
	1.26	02	—
	2.05	13	2.03
	2.55	04	2.52
	3.22	15	3.23
	3.80	06	3.78
	1.48	20	1.48
$a = 5.99 \text{ nm}, b = 7.01 \text{ nm}$			
(b) <b>B2</b> Col <sub>obl</sub>	$\theta_{\text{exp}}$	$hk$	$\theta_{\text{cal}}$
	0.97	10	—
	1.26	01	—
	2.05	11	2.04
	2.55	02	2.53
	3.22	12	3.29
	3.80	03	3.79
	1.48	2-1	—
$a = 5.96 \text{ nm}, b = 4.54 \text{ nm}, \gamma = 130^\circ$			
(c) <b>B6</b> Col <sub>rec</sub>	$\theta_{\text{exp}}$	$hk$	$\theta_{\text{cal}}$
	0.161	11	—
	1.11	02	—
	1.28	22	1.22
	1.66	13	1.68
	2.25	04	2.22
	2.80	15	2.79
	3.37	06	3.33
	2.20	24	2.28
	3.31	26	3.37
	1.79	33	1.83
	2.82	35	2.88
	0.51	20	0.51
	1.05	40	1.01
	1.52	42	1.50
	$a = 17.45 \text{ nm}, b = 7.96 \text{ nm}$		

amplitude of the density modulation perpendicular to the layer normal in the substances under consideration caused by an alternating change between fluorinated and non-fluorinated regions. Table 2(c) displays, besides the sketch of the observed pattern, the cell parameters calculated on the basis of the positions of the reflections of the powder-like pattern.

But the arrangement of the molecules must be different in comparison with that in the columnar structure of the second group. This is indicated by the phase transition enthalpy SmA-Col<sub>rec</sub> (figure 1) which is more than one order of magnitude higher ( $10 \text{ J g}^{-1}$ ) than the phase transition enthalpy SmC-Col ( $0.25 \text{ J g}^{-1}$ ). Furthermore, the  $d$ -values decrease discontinuously at the SmA/Col<sub>rec</sub>

a) SmA phase (B2)

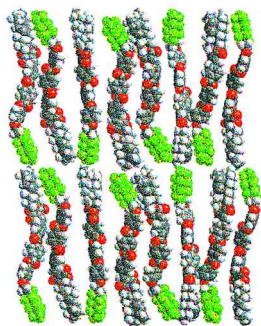
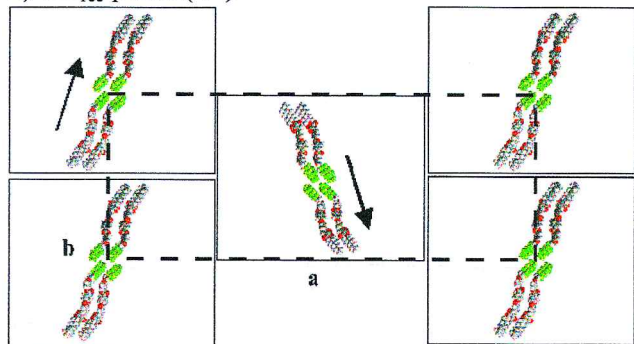
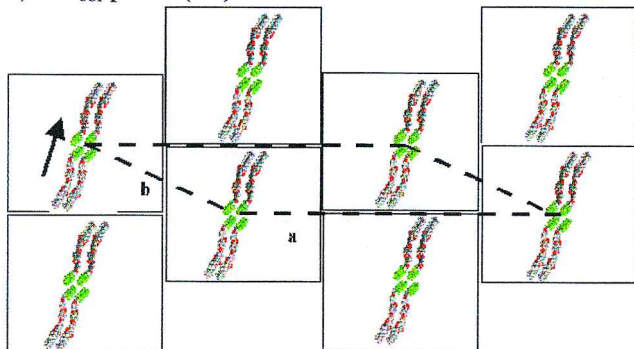
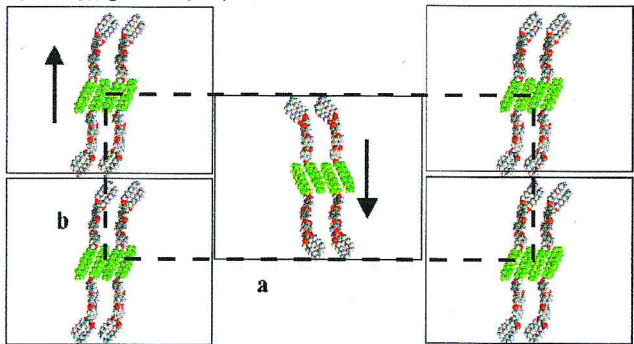
b) Col<sub>rec</sub> phase (B2)c) Col<sub>obl</sub> phase (B2)d) Col<sub>rec</sub> phase (B6)

Figure 5. Structural models (designed by the Cerius 2 program) of the SmA (a) and columnar (b–d) phases. The models shown in (b) and (c) correspond to the alternative interpretations of the X-ray pattern according to table 2 (a) and 2 (b).

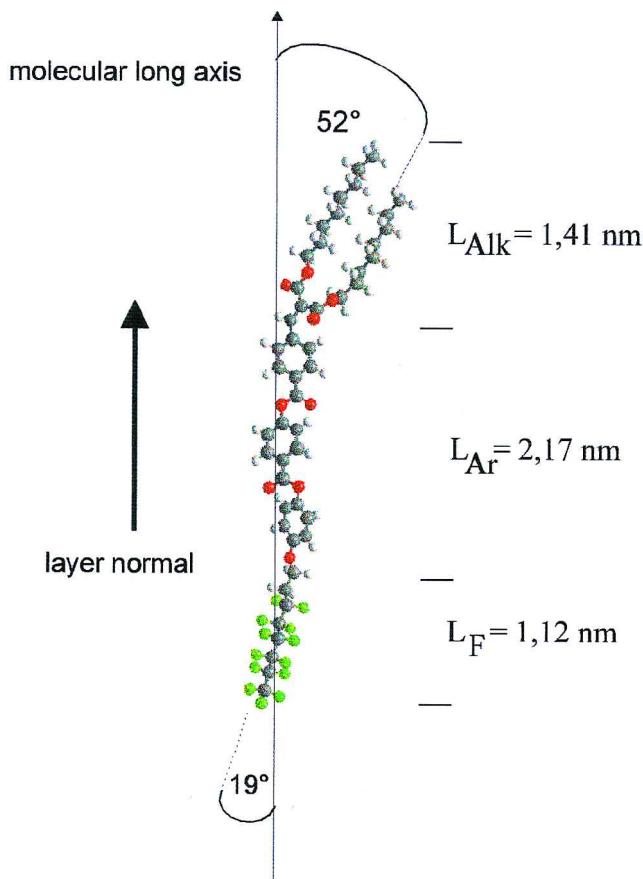


Figure 9. Schematic model of the tilt of molecular moieties with respect to the layer normal in the SmA phase of compound **B2**.

transition indicating a reorganization of the packing [figure 4 (c)]. Though the diffuse outer scattering at the equator proves the perpendicular alignment of the molecules in the SmA phase as well as in the Col<sub>rec</sub> phase, the  $d$ -value in the Col<sub>rec</sub> phase does not correspond to the length of the molecule.

The outer diffuse scattering is changed at the transition into the low temperature phase. In the columnar phase it consists of two diffuse scattering maxima at  $8.7^\circ$  and  $10^\circ$  [figure 6 (b)]. The FWHM of the first diffuse scattering is much smaller in the case of the columnar phase than that of the second diffuse scattering, in contradiction to that of the compounds in the second group [figure 6 (a)], but the coherence length of the lateral packing remains of short range order. The difference between the  $d$ -value and the length of the perpendicularly aligned molecules demands a model in which the building groups of the two-dimensional cell (fragments of layers) consist of antiparallel aligned molecules which are shifted with respect to each other so that the perfluorinated parts are together [figure 5 (d)]. This leads to a higher ordered packing in

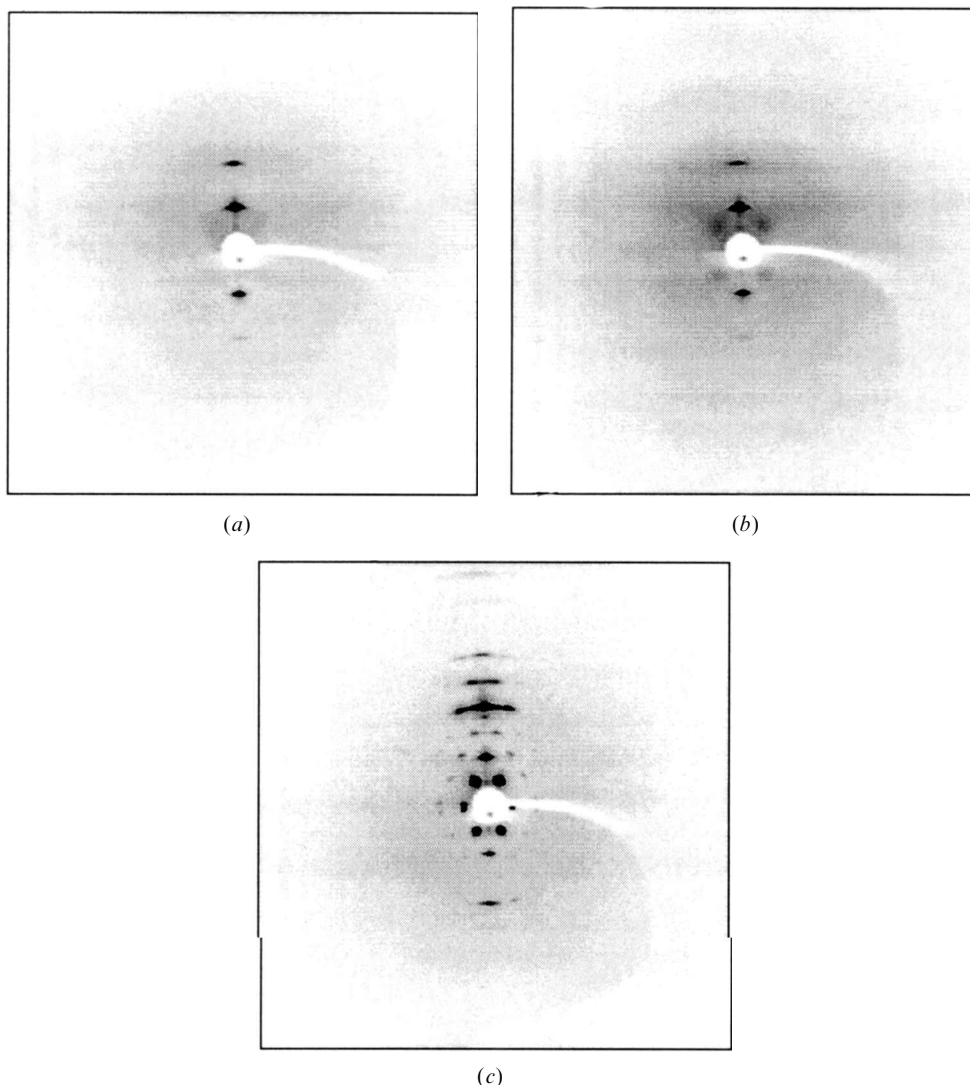


Figure 10. X-ray pattern of the small angle region of the oriented sample of compound **B6**. SmA phase at 140°C (a); SmA phase at 120°C (b); Col<sub>rec</sub> phase at 100°C (c).

the perfluorinated sub-layer in comparison with that of the Col phase in the second group, which is indicated by the smaller FMHW of the corresponding scattering. In this way the incompatible parts of the molecules are separated, again.

#### 4. Conclusion

The substances under consideration show the influence of steric interaction on the one hand and repulsion caused by chemically incompatible segments on the other. In the first group of compounds investigated the steric interaction clearly dominates the structure so that only an antiparallel packing of the molecules results. In the second and third groups the influence of the incompatibility is more and more enhanced. As a consequence, columnar structures arise in which the

incompatible parts are separated on a microscopic scale. Two types of columnar structure have been observed which are distinguished by the tilt of the molecules (zero or  $\cong 29^\circ$ ) within the blocks.

We thank the Deutsche Forschungsgemeinschaft (Project Di 465/3-1) as well as the Fond der Chemischen Industrie for financial support of our liquid crystal work.

#### References

- [1] MAHLER, W., GUILLON, D., and SKOULIOS, A., 1985, *Mol. Cryst. liq. Cryst. Lett.*, **2**, 111.
- [2] VINEY, C., RUSSELL, T. P., DEPERO, L. E., and TWIEG, R. J., 1989, *Mol. Cryst. liq. Cryst.*, **168**, 63.
- [3] VINEY, C., TWIEG, R. J., RUSSELL, T. P., and DEPERO, L. E., 1989, *Liq. Cryst.*, **5**, 1783.

- [4] RABOLT, J. F., RUSSELL, T. P., and TWIEG, R. J., 1984, *Macromolecules*, **17**, 2786.
- [5] HÖPKEN, J., and MÖLLER, M., 1992, *Macromolecules*, **25**, 2485.
- [6] TURBERG, P. M., and BRADY, E., 1988, *J. Am. chem. Soc.*, **110**, 7797.
- [7] NGUYEN, H. T., SIGAUD, G., ACHARD, M. F., HARDOUIN, F., TWIEG, R. T., and BETTERTON, K., 1991, *Liq. Cryst.*, **10**, 389.
- [8] JANULIS, E. P., NOVACK, J. C., PAPAPOLYMEROU, G. A., TRISTANI-KENDRA, M., and HUFFMAN, W. A., 1988, *Ferroelectrics*, **85**, 375.
- [9] TWIEG, R., BETTERTON, K., DIPIETRO, R., GRAVERT, D., NGUYEN, C., NGUYEN, H. T., BABEAU, A., DESTRADE, C., and SIGAUD, G., 1992, *Mol. Cryst. liq. Cryst.*, **217**, 201.
- [10] TOURNILHAC, F., BOSIO, L., SIMON, J., BLINOV, L. M., and YABLONSKY, S. V., 1993, *Liq. Cryst.*, **14**, 405.
- [11] BLINOV, L. M., and TOURNILHAC, F., 1993, *Ferroelectrics*, **148**, 111.
- [12] TOURNILHAC, F., BLINOV, L. M., SIMON, J., SUBACHIES, D. B., and YABLONSKY, S. Y., 1993, *Synth. Met.*, **54**, 253.
- [13] TOURNILHAC, F., and SIMON, J., 1991, *Ferroelectrics*, **114**, 283.
- [14] BLINOV, L. M., LOBKO, T. A., OSTROVSKII, B. I., SULIANOV, S. N., and TOURNILHAC, F., 1993, *J. Phys. II Fr.*, **3**, 1121.
- [15] PAVLUCHENKO, A. I., SMIRNOVA, N. I., PETROV, V. F., FIALKOV, Y. A., SHELYAZHENKO, S. V., and YAGUPOLSKY, L. M., 1991, *Mol. Cryst. liq. Cryst.*, **209**, 225.
- [16] OSTROVSKII, B. I., 1993, *Liq. Cryst.*, **14**, 131.
- [17] RIEKER, P., and JANULIS, E. P., 1995, *Phys. Rev. E*, **52**, 2688.
- [18] LOBKO, T. A., OSTROVSKII, B. I., PAVLUCHENKO, A. I., and SULIANOV, S. N., 1993, *Liq. Cryst.*, **15**, 361.
- [19] KODEN, M., NAKAGAWA, K., ISHII, Y., FUNADA, F., MATSUURA, M., and AWANE, K., 1989, *Mol. Cryst. liq. Cryst. Lett.*, **6**, 185.
- [20] DOI, T., TAKENAKA, S., KUSABAYASHI, S., NISHIHATA, Y., and TERAUCHI, H., 1991, *J. mater. Chem.*, **1**, 169.
- [21] DIELE, S., LOSE, D., KRUTH, H., PELZL, G., GUITTARD, F., and CAMBON, A., 1996, *Liq. Cryst.*, **21**, 603.
- [22] KROMM, P., COTRAIT, M., ROUILLON, J. C., BAROIS, P., and NGUYEN, H. T., 1996, *Liq. Cryst.*, **21**, 121.
- [23] HARDOUIN, F., LEVELUT, A. M., ACHARD, M., and SIGAUD, G., 1983, *J. Chim. phys.*, **80**, 53.
- [24] DE GENNES, P. G., and PROST, J., 1995, *The Physics of Liquid Crystals* (Oxford: Clarendon Press).
- [25] PROST, J., and BAROIS, P., 1983, *J. Chim. Phys.*, **80**, 65.
- [26] DERZHANSKI, A., and PETROV, G., 1987, *Mol. Cryst. liq. Cryst.*, **151**, 303.
- [27] DERZHANSKI, A., and PETROV, G., 1982, *Mol. Cryst. liq. Cryst.*, **89**, 339.
- [28] DIELE, S., MÄDICKE, A., KNAUFT, K., NEUTZLER, J., WEISSFLOG, W., and DEMUS, D., 1991, *Liq. Cryst.*, **10**, 47.
- [29] GÖRING, P., PELZL, G., DIELE, S., DELAVIER, D., and SIEMENSMEIER, K., 1995, *Liq. Cryst.*, **19**, 629.
- [30] DIETZMANN, E., WEISSFLOG, W., MARKSCHEFFEL, S., JAKLI, A., LOSE, D., and DIELE, S., 1996, *Ferroelectrics*, **180**, 341.
- [31] KRESSE, H., RABENSTEIN, P., STETTIN, H., DIELE, S., DEMUS, D., and WEISSFLOG, W., 1988, *Cryst. Res. Technol.*, **23**, 135.
- [32] WEISSFLOG, W., WIEGELEBEN, A., DIELE, S., and DEMUS, D., 1984, *Crystal. Res. Technol.*, **19**, 583.
- [33] HILDEBRAND, J. H., and SCOTT, R. L., 1962, *Regular Solutions* (Englewood Cliffs, NJ: Prentice-Hall, Inc.).
- [34] YOUNG, C. L., 1969, *Trans. Faraday Soc.*, **65**, 2639.
- [35] SCOTT, R. L., 1958, *J. phys. Chem.*, **62**, 136.
- [36] DORSET, D. L., 1977, *Chem. Phys. Lipids*, **20**, 13.
- [37] CLARK, E. S., and MUUS, L. T., 1962, *Z. Kristallogr.*, **117**, 119.
- [38] DE SANTIS, P., GIGLIO, E., LIQUORI, A. M., and RIPAMONDI, A., 1963, *J. Polym. Sci.*, **A1**, 1383.
- [39] SKOULIOS, A., 1967, *Adv. Colloid Interface Sci.*, **1**, 79.
- [40] BRANDUP, J., and IMMERGUT, E. H., 1975, *Polymer Handbook* (Wiley and Sons).
- [41] BUNN, C. W., and HOWELLS, E. R., 1954, *Nature*, **174**, 549.
- [42] STROBL, G. R., 1977, *J. Polym. Sci. Polym. Symp.*, **59**, 121.
- [43] STROBL, G. R., SCHWICKERT, H., and TRZEBIATOWSKI, T., 1983, *Ber. Bunsenges. phys. Chem.*, **87**, 274.
- [44] JOHANSSON, G., PERCEC, V., UNGAR, G., and SMITH, K., 1997, *Chem. Mater.*, **9**, 164.
- [45] KROMM, P., COTRAIT, M., and NGUYEN, H. T., 1996, *Liq. Cryst.*, **21**, 95.